Biomaterials 30 (2009) 242–253

Contents lists available at ScienceDirect

Biomaterials

journal homepage: www.elsevier.com/locate/biomaterials

Biodegradable amphiphilic poly(ethylene oxide)-*block*-polyesters with grafted polyamines as supramolecular nanocarriers for efficient siRNA delivery

Xiao-Bing Xiong [a], Hasan Uludağ [b], Afsaneh Lavasanifar [a,*]

[a] Faculty of Pharmacy and Pharmaceutical Sciences, University of Alberta, Edmonton, Alberta, Canada T6G 2N8
[b] Department of Chemical and Materials Engineering, Faculty of Engineering, University of Alberta, Edmonton, AB, T6G 2G6 Canada

ARTICLE INFO

Article history:
Received 30 June 2008
Accepted 2 September 2008
Available online 5 October 2008

Keywords:
Micelles
siRNA delivery
Block polymer
Poly(ethylene oxide)-*b*-poly(ε-caprolactone)
Polyamine
Multidrug resistance

ABSTRACT

The RNA interference (RNAi) technology has been successfully used in elucidating mechanisms behind various biological events. However, in the absence of safe and effective carriers for *in vivo* delivery of small interfering RNAs (siRNAs), application of this technology for therapeutic purposes has lagged behind. The objective of this research was to develop promising carriers for siRNA delivery based on degradable poly(ethylene oxide)-*block*-polyesters containing polycationic side chains on their polyester block. Toward this goal, a novel family of biodegradable poly(ethylene oxide)-*block*-poly(ε-caprolactone) (PEO-*b*-PCL) based copolymers with polyamine side chains on the PCL block, i.e., PEO-*b*-PCL with grafted spermine (PEO-*b*-P(CL-*g*-SP)), tetraethylenepentamine (PEO-*b*-P(CL-*g*-TP)), or *N*,*N*-dimethyldipropylenetriamine (PEO-*b*-P(CL-*g*-DP)) were synthesized and evaluated for siRNA delivery. The polyamine-grafted PEO-*b*-PCL polymers, especially PEO-*b*-P(CL-*g*-SP), demonstrated comparable toxicity to PEO-*b*-PCL *in vitro*. The polymers were able to effectively bind siRNA, self-assemble into micelles, protect siRNA from degradation by nuclease and release complexed siRNA efficiently in the presence of low concentrations of polyanionic heparin. Based on flow cytometry and confocal microscopy, siRNA formulated in PEO-*b*-P(CL-*g*-SP) and PEO-*b*-P(CL-*g*-TP) micelles showed efficient cellular uptake through endocytosis by MDA435/LCC6 cells transfected with *MDR-1*, which encodes for the expression of P-glycoprotein (P-gp). The siRNA formulated in PEO-*b*-P(CL-*g*-SP) and PEO-*b*-P(CL-*g*-TP) micelles demonstrated effective endosomal escape after cellular uptake. Finally, *MDR-1*-targeted siRNA formulated in PEO-*b*-P(CL-*g*-SP) and PEO-*b*-P(CL-*g*-TP) micelles exhibited efficient gene silencing for P-gp expression. The results of this study demonstrated the promise of novel amphiphilic PEO-*b*-P(CL-*g*-polyamine) block copolymers for efficient siRNA delivery.

1. Introduction

RNA interference (RNAi) represents a promising gene silencing technology for functional genomics and a potential therapeutic strategy for a variety of genetic diseases [1–3]. The use of small interference RNA (siRNAs) in gene therapy research has surged over the past years following the discovery that the RNAi mechanism of gene-specific silencing can be exploited in human disease therapy [4,5]. However, due to the large molecular weight, negative charge of siRNA duplexes, and the susceptibility to enzymatic degradation, the effective cellular uptake and intracellular delivery of siRNA for clinical application represent a major challenge for widespread use of RNAi as a therapeutic modality or even as an investigational tool *in vivo* [6–8].

Successful development of RNAi for clinical application is dependent on the discovery of safe and effective carriers [7,9]. In general, the ideal carrier for siRNA should be able to bind and condense siRNA, provide protection against degradation, specifically direct siRNA to target cells, facilitate its intracellular uptake, escape from endosome/lysosome into cytosol, and finally promote efficient gene silencing. Polymeric carriers have been of interest for siRNA delivery because they could be chemically engineered to meet all or some of these requirements simultaneously [4,10]. Among different polymers designed for siRNA delivery, the micelle assembling block copolymers consisting of poly(ethylene oxide) (PEO) and polycation segment such as polyethylenimine (PEI) and poly(L-lysine) (PLL) have been emerging as promising carriers. These polymers are displaying properties suitable for *in vivo* siRNA delivery, including siRNA

* Corresponding author. Tel.: +1 780 492 2742; fax: +1 780 492 1217.
E-mail address: alavasanifar@pharmacy.ualberta.ca (A. Lavasanifar).

0142-9612/$ – see front matter © 2008 Elsevier Ltd. All rights reserved.
doi:10.1016/j.biomaterials.2008.09.025

binding and condensation, self-assembly into poly-ion complex (PIC) micelles with a diameter around 100 nm, avoiding recognition by reticuloendothelial systems (RES), increasing nuclease resistance and tolerance under physiological conditions [11–15]. However, the safety profile of these polymers containing large polycationic segments and their non-biodegradable nature in some cases (e.g., PEI containing polymers) remain an obstacle for clinical application. In this regard, development of siRNA carriers based on biomaterials with a more proven safety record is desirable.

Copolymers with PEO as the shell-forming block and polyester as the core-forming block, such as PEO-*b*-P(ε-caprolactone) (PEO-*b*-CL), PEO-*b*-polylactide (PEO-*b*-PLA) and PEO-*b*-P(lactide-*co*-glycolide) (PEO-*b*-PLGA), are more-established biomaterials for drug delivery [16–18]. The biocompatibility of both the PEO and the polyester block has been demonstrated. PEO has been extensively used for coating different pharmaceuticals to modify their pharmacokinetics, increase their safety or lower their immunogenicity [19,20]. Polyesters are proven biodegradable polymers and have a history of safe application in absorbable biomedical devices such as sutures [21,22]. However, the lack of cationic moieties in PEO or polyester blocks limits their usefulness for gene or siRNA delivery [23]. In this study, we reported on the synthesis of a novel family of PEO-*b*-polyester copolymers grafted with short cationic moieties on polyester segments and explored their safety and potential for the formation of PIC micelles for efficient siRNA delivery.

2. Materials and methods

2.1. Materials

Diisopropyl amine (99%), benzyl chloroformate (tech. 95%), sodium (in kerosin), butyl lithium (Bu-Li) in hexane (2.5 M solution), 3,3-diethoxy-1-propanol (DEP), naphthalene, ethylene oxide (EO), branched PEI (25 kDa), *N*,*N*-dicylcohexyl carbodiimide (DCC), *N*-hydroxysuccinimide (NHS), pyrene, spermine (SP), tetraethlyenepentamine (TP), and *N*,*N*-dimethyldipropylenetriamine (DP) were purchased from Sigma Chemicals (St. Louis, MO, USA). ε-Caprolactone was purchased from Lancaster Synthesis (Heysham, UK) and distilled by calcium hydride before use. Stannous octoate was purchased from MP Biomedicals Inc. (Eschwege, Germany). Potassium naphthalene solution was prepared by conventional method and the concentration was determined by titration [24]. The scrambled siRNA (Silencer® Negative siRNA and Silencer® FAM™-labeled Negative siRNA) and the anti-*MDR-1* siRNA (*MDR-1* siRNA) were purchased from Ambion (Austin, TX). Cell culture media RPMI 1640, penicillin–streptomycin, fetal bovine serum, L-glutamine and HEPES buffer solution (1 M) were purchased form GIBCO, Invitrogen Corp (USA). All other chemicals were reagent grade. MDA435/LCC6 cells transfected with *MDR-1* overexpressing P-glycoprotein (P-gp) on their cell membrane, were a gift from the laboratory of Dr. Clarke (Georgetown University Medical School, Washington, DC) [25,26]. Cells were grown as adherent cultures and maintained in RPMI 1640 supplemented with 10% fetal bovine serum at 37 °C and 5% CO_2.

2.2. Synthesis of PEO-b-PCL with grafted polyamine

Poly(ethylene oxide)-*b*-poly(ε-caprolactone-*g*-polyamine) (PEO-*b*-P(CL-*g*-polyamine)) block copolymers were prepared from PEO-*b*-poly(α-carboxyl-ε-caprolactone) (PEO-*b*-PCCL). The synthesis of PEO-*b*-PCCL has been described in detail previously [27]. Briefly, PEO-*b*-poly(α-benzyl carboxylate-ε-caprolactone) (PEO-*b*-PBCL) block copolymer was synthesized by ring-opening polymerization of α-benzylcarboxylate-ε-caprolactone (BCL) using α-methoxy-PEO (PEO) as an initiator ($M_n = 5000\ g\ mol^{-1}$, $M_w/M_n = 1.05$). Then protective benzyl group of the benzyl-substituted units were removed by the catalytic debenzylation of PEO-*b*-PBCL in the presence of H_2 to obtain PEO-*b*-PCCL. Then, active ester method was used to attach pendant polyamine groups to the polyester section by the amide bond formation using NHS/DCC catalyst system (Scheme 1). In a typical process, PEO-*b*-PCCL (200 mg, ~0.01 mmol) was dissolved in 10 mL of dry THF. After addition of DCC and NHS in THF, the solution was stirred for 2 h until a precipitate was formed. The precipitate was removed by filtration. The polyamines, SP, TP, and DP, were dissolved in THF and added drop-wise to the polymer solution. The reaction proceeded for another 24 h under stirring at room temperature. The resulting solution was centrifuged to remove the precipitate followed by evaporation under vacuum to remove the solvents. Methanol (10 mL) was introduced to dissolve the product. The resulting solution was then dialyzed (molecular weight cut-off of 3500 Da) extensively against water and the polymer solution was freeze-dried for further use.

The composition of the reaction products was determined by a 300 MHz ^1H NMR spectroscope (Bruker 300 AM; Billerica MA). The solvent used for ^1H NMR was D_2O for PEO-*b*-P(CL-*g*-SP), PEO-*b*-P(CL-*g*-TP) and $CDCl_3$ for PEO-*b*-P(CL-*g*-DP), respectively. The polyamine substitution level and the molecular weight of the synthesized copolymers were estimated based on peak intensity ratio of the methylene protons from polyamine (–CH_2–NH–) and PEO (–CH_2CH_2O–). The compositions of the synthesized PEO-*b*-P(CL-*g*-polyamine) copolymers were also confirmed by infra-red (IR) spectroscopy using a Nicolet Magna-IR 550 Spectrophotometer (WI, USA).

2.3. Cytotoxicity

The cytotoxicity of various PEO-*b*-P(CL-*g*-polyamine) copolymers against *MDR-1*-transfected MDA435/LCC6 cells was evaluated using the 3-(4,5-dimethylthiazol-2-yl)-2,5-diphenyltetrazolium bromide (MTT) assay. MDA435/LCC6 cells (4000 cells/well) were seeded into 96-well plates. After overnight incubation, the culture medium was replaced with 200 μL serial diluted solutions of the polymers, and the wells were incubated for another 48 h. Then, 20 μL of MTT stock solution in phosphate buffered saline (PBS) was added to each well. After 3 h, medium was aspirated and the precipitated formazan was dissolved in 200 μL of DMSO. Cell viability was determined by measuring the optical absorbance differences between 570 and 650 nm using a PowerwaveX340 microplate reader (BIO-TEK Instruments, Inc. VT, USA). The relative cell growth % related to the control containing cell culture medium without polymer was calculated by $[A]_{test}/[A]_{control} \times 100$. All the tests were performed in triplicate. The concentration of drugs leading to 50% cell growth inhibition (IC_{50}) was estimated from the plot of the percentage of viable cells versus log DOX concentration for each treatment.

2.4. Haemolysis assay

The synthesized PEO-*b*-P(CL-*g*-polyamine) copolymers, PEI and Triton X-100 (1%, w/v) were dissolved in PBS (pH 7.4). Using blood obtained from a male Sprague-Dawley rat by cardiac puncture, erythrocytes were isolated by centrifugation at

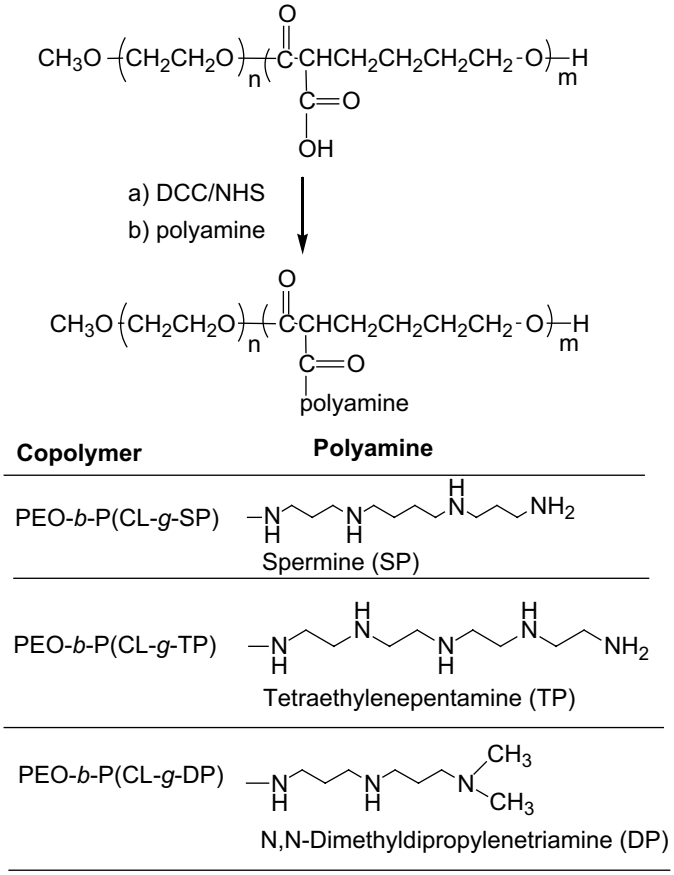

Scheme 1. Synthetic procedure for the preparation of PEO-*b*-PCL with grafted SP, TP and DP.

1500 g for 10 min at 4 °C. The cell pellet was resuspended to obtain a 2% (w/v) erythrocyte suspension with pre-chilled PBS, and then added into a 96-well plate (100 μL/well). 100 μL of test samples were then added to the erythrocyte suspension in the multiwell plate which was incubated at 37 °C for 1 h. The supernatant from each sample was removed to a new plate and the absorbance was measured at 550 nm using a microplate reader. The haemolysis % of each polymer was estimated by comparing their absorbance to that from Triton X-100 treatment, which led to 100% haemolysis and was used as the positive control.

2.5. Determination of siRNA binding by gel retardation assay

The siRNA binding ability of the PEO-*b*-P(CL-*g*-polyamine) copolymers was analyzed by agarose gel electrophoresis [28]. The PEO-*b*-P(CL-*g*-polyamine)/siRNA complexes were prepared by mixing 8 μL of 0.1 M HEPES buffer (pH 6.5) with 4 μL of negative siRNA (containing 2 μg siRNA) and 8 μL of serially-diluted concentrations of a PEO-*b*-P(CL-*g*-polyamine) solution (containing polymers ranging from 1 to 64 μg) and incubated for 30 min at 37 °C. The mixture was incubated for ~30 min at 37 °C, after which 4 μL of 6× sample buffer (50% glycerol, 1% bromophenol blue, and 1% cylene cyenol FF in TBE buffer) was added, and the samples were loaded onto 2% agarose gels containing 0.05 mg/mL ethidium bromide (EtBr). Electrophoresis was performed at 130 mV and ~52 mA for 15 min, and the resulting gels were photographed under UV-illumination. The pictures were digitized and analyzed with Scion image analysis software to determine the mean density of siRNA bands. The binding percentage was calculated based on the relative intensity of free siRNA band in each well with respect to wells with free siRNA (i.e., in the absence of any polymers). The binding for each polymer was tested at least in 2 independent experiments.

2.6. siRNA release by polyanion competition

The ability of complexes to release siRNA after a challenge with the competing polyanionic heparin was determined as a measure of complex stability [29]. Complexes were prepared at polymer:siRNA mass ratio of 32:1 to ensure complete binding of siRNA by the polymers, and then incubated with 0.78, 1.52, 3.04, 6.08, 12.48, and 24.32 μg of heparin sulfate at 37 °C for 1 h. The solutions were run on agarose gel as described earlier. Results were presented as average of at least 2 independent experiments.

2.7. Serum stability study

To determine the protective role of the polymers against siRNA degradation, PEO-*b*-P(CL-*g*-polyamine)/siRNA PIC micelles were prepared at several polymer:siRNA weight ratios, ranging from 4:1 to 32:1 and incubated with 25% fetal bovine serum (FBS) for 24 h at 37 °C. At the same time, free siRNA and PEI/siRNA (1:1 in weight ratio) were incubated with 25% FBS at 37 °C for 24 h as the negative and positive controls, respectively. Samples were then incubated for 1 h with excess of heparin to ensure complete release of siRNA from the formulation. The intact siRNA percentage was then analyzed by agarose gel electrophoresis as described earlier. The results shown represent an average of at least 3 independent experiments.

2.8. Characterization of the self-assembly of PEO-b-P(CL-g-polyamine)/siRNA PIC micelles

A change in the fluorescence excitation spectra of pyrene in the presence of varied concentrations of PEO-*b*-P(CL-*g*-polyamine) block copolymers was used to determine the critical micellar concentration (CMC) according to the method described previously [30]. To determine the particle size and ζ-potential, copolymer/siRNA PIC micelles were prepared at 32:1 of copolymer:siRNA weight ratio. PEI/siRNA complex was prepared at 1:1 weight ratio for this analysis. Their average diameters and size distributions were estimated by dynamic light scattering (DLS) using Malvern Zetasizer 3000 at 25 °C. Zeta-potential of the prepared complex was also evaluated by the laser-doppler electrophoresis method using Zetasizer 3000.

2.9. siRNA uptake study by flow cytometry

To assess the ability of polymers to transfer siRNA into *MDR-1*-transfected MDA435/LCC6 cells, carboxyfluorescein (FAM)-labeled siRNA was formulated in the PIC micelles of different PEO-*b*-P(CL-*g*-polyamine) copolymers at 32:1 of polymer:siRNA weight ratio or in PEI at 1:1 weight ratio according to the above-mentioned method. MDA435/LCC6 cells in 6-well plates (5×10^4 cells per well) were pulsed with PICs containing 100 nM of siRNA. After incubation for 3 h, the cells were washed with cold PBS, trypsinized and the uptake of FAM-labeled siRNA was detected by a Becton–Dickinson FACSort™ flowcytometer (Franklin Lakes, NJ). The data were analyzed with CellQuest™ software (Becton–Dickinson).

2.10. siRNA uptake and cellular distribution study by confocal microscopy

Confocal fluorescent microscopy was used to assess the intracellular trafficking of siRNA. FAM-labeled siRNA was complexed with PEO-*b*-P(CL-*g*-SP), PEO-*b*-P(CL-*g*-TP), PEO-*b*-P(CL-*g*-DP) in the weight ratio of 32:1 or PEI in the weight ratio of 1:1. Cells grown on the glass coverslips in a 12-well plate were incubated with the complexes for 1 and 3 h. At the end of incubation period, the cells were washed three times with PBS, fixed in paraformaldehyde in PBS for 10 min. For nucleus labeling, fixed cells were washed with PBS and then incubated with DAPI (Molecular Probes, Invitrogen Co., OR, USA) for 15 min. To observe the intracellular distribution of the PIC micelles, cells were incubated with LysoTracker Red (50 nM, Molecular Probe, Invitrogen Co., OR, USA) for 0.5 h at the end of uptake study for endosome/lysosome labeling. The cells were then washed three times with PBS and stored at 4 °C. Localization of complexes in cells was visualized by a Zeiss 510 LSMNLO confocal microscope (Carl Zeiss Microscope systems, Jena, Germany) with identical settings for each confocal study.

2.11. Transfection of MDR-1-targeted siRNA to silence P-glycoprotein (P-gp) expression

MDR-1 siRNA was complexed with PEO-*b*-P(CL-*g*-SP) and PEO-*b*-P(CL-*g*-TP) at a mass ratio of 32:1 (polymer:siRNA) or PEI at mass ratio of 1:1 as previously described. *MDR-1*-transfected MDA435/LCC6 cells (4000 cells/well) were seeded into an 8-well plate and incubated overnight for attachment. The prepared siRNA/polymer complexes were added and incubated with the cells at siRNA concentrations of 100, 200 and 300 nM for another 48 h at 37 °C. The cells were washed with PBS, trypsinized and resuspended in 500 μL of 5% BSA in PBS, and incubated with FITC-labeled anti-human P-gp antibody (20 μL) for 30 min at 4 °C. After that, cells were washed three times with cold PBS buffer, and the P-gp level was measured by a Becton–Dickinson FACSort™ flowcytometer. The RNAi effect was also observed by confocal microscopy. Toward this, cells grown on coverslips were treated with *MDR-1* siRNA/polymer complexes (300 nM) for 48 h at 37 °C, washed with fresh media and incubated with FITC-labeled anti-human P-gp antibody (20 μL/1 mL) for another 30 min at 4 °C. The cells were then washed three times with PBS, fixed in paraformaldehyde in PBS for 10 min, treated with DAPI for nuclei staining, and examined by confocal microscopy.

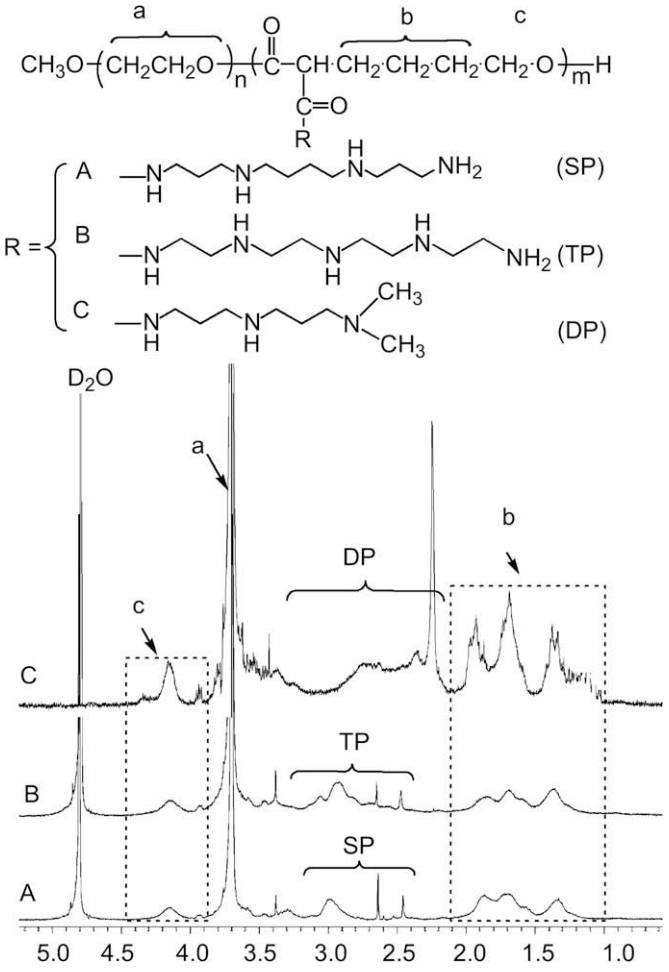

Fig. 1. ^{1}H NMR of (A) PEO-*b*-P(CL-*g*-SP), (B) PEO-*b*-P(CL-*g*-TP) in D_2O and (C) PEO-*b*-P(CL-*g*-DP) in $CDCl_3$.

3. Results

3.1. Synthesis and characterization of PEO-b-PCL with grafted polyamine groups

The PEO-*b*-P(CL-*g*-SP), PEO-*b*-P(CL-*g*-TP) and PEO-*b*-P(CL-*g*-DP) were synthesized from NHS-activated PEO-*b*-PCCL (Scheme 1). The final structure of copolymer was confirmed by ^{1}H NMR (Fig. 1) and IR (Fig. 2). The characteristics of prepared block copolymers are shown in Table 1. Peaks corresponding to specific polyamine groups of SP, TP and DP were observed at 2.1–3.2 ppm in the ^{1}H NMR spectra, indicating the successful conjugation of polyamine groups to block copolymers (Fig. 1). Based on the intensity ratio of proton peak for the polyamine groups (–NHCH_2–, δ 2.1–3.2) to that for the PCL segment (OC–$(CH_2)_4$–CH_2O–, δ 4.05), the polyamine substitution levels of the copolymer were calculated at ~48, ~50 and ~80% for PEO-*b*-P(CL-*g*-SP), PEO-*b*-P(CL-*g*-TP) and PEO-*b*-P(CL-*g*-DP), respectively. Successful synthesis of PEO-*b*-P(CL-*g*-polyamine)s was also confirmed by IR spectra (Fig. 2). PEO-*b*-P(CL-*g*-SP) and PEO-*b*-P(CL-*g*-TP), which contain primary and secondary amine groups in their structures showed N–H stretch at ~3260 and 3400 cm^{-1}, while PEO-*b*-P(CL-*g*-DP) which contains secondary and tertiary amine groups, showed N–H stretch at ~3260 cm^{-1}. The CMC of PEO-*b*-P(CL-*g*-polyamine) polymers (1.95–3.65 μM) was determined to be significantly higher than that of PEO-*b*-PCL (0.19 μM), but lower than that of PEO-*b*-PCCL (12.2 μM). Conjugation of the more hydrophobic polyamine DP to PEI-*b*-PBCL led to a copolymer with a lower CMC value as compared to PEO-*b*-P(CL-*g*-SP) and PEO-*b*-P(CL-*g*-TP) (Table 1).

3.2. Cytotoxicity and haemolysis study

Cytotoxicity of synthesized PEO-*b*-P(CL-*g*-polyamine)s was evaluated in *MDR-1*-transfected MDA435/LCC6 cells using the MTT assay (Fig. 3A). Compared to PEI (IC_{50}, 6.58 μg/mL), PEO-*b*-P(CL-*g*-SP), PEO-*b*-P(CL-*g*-TP) and PEO-*b*-P(CL-*g*-DP) showed significant lower cytotoxicity against MDA435/LCC6 cells with IC_{50} values of 452, 165, and 130 μg/mL, respectively. Compared to PEO-*b*-PCL (IC_{50} > 500 μg/mL), PEO-*b*-P(CL-*g*-TP) and PEO-*b*-P(CL-*b*-DP) were more cytotoxic, whereas grafting of the endogenous polyamine SP to the PCL block didn't increase the cytotoxicity of PEO-*b*-PCL significantly. The polyamine-grafted copolymers did not display a significant haemolytic activity even at highest polymer concentration of 1 mg/mL (<1%). Compared to these copolymers, PEI showed dose-dependent haemolysis up to 4% under our experimental conditions (Fig. 3B).

Table 1
Characteristics of PEO-*b*-P(CL-*g*-polyamine) polymers and the prepared polymer/siRNA PIC micelles

Polymer[a]	Polymer M_n[b] (g mol^{-1})	CMC[c] (μM)	Average diameter (nm)	ζ-potential (mV)
PEO_{114}-*b*-P(CL-*g*-SP)$_{12-6}$	8300	3.15 ± 0.22	56.8 ± 4.2	2.50 ± 0.36
PEO_{114}-*b*-P(CL-*g*-TP)$_{12-6}$	8500	3.65 ± 0.18	65.4 ± 4.2	2.27 ± 0.12
PEO_{114}-*b*-P(CL-*g*-DP)$_{12-9}$	9170	1.95 ± 0.22	90.5 ± 3.2	3.33 ± 0.90

[a] The first subscript number stands for the polymerization degree of each block and the second one stands for the number of repeated unit with substituted polyamine groups based on ^{1}H NMR analysis.
[b] Determined by ^{1}H NMR.
[c] Measured from the onset of a rise in the intensity ratio of peaks at 339 nm to peaks at 334 nm in the fluorescence excitation spectra of pyrene plotted versus logarithm of polymer concentration.

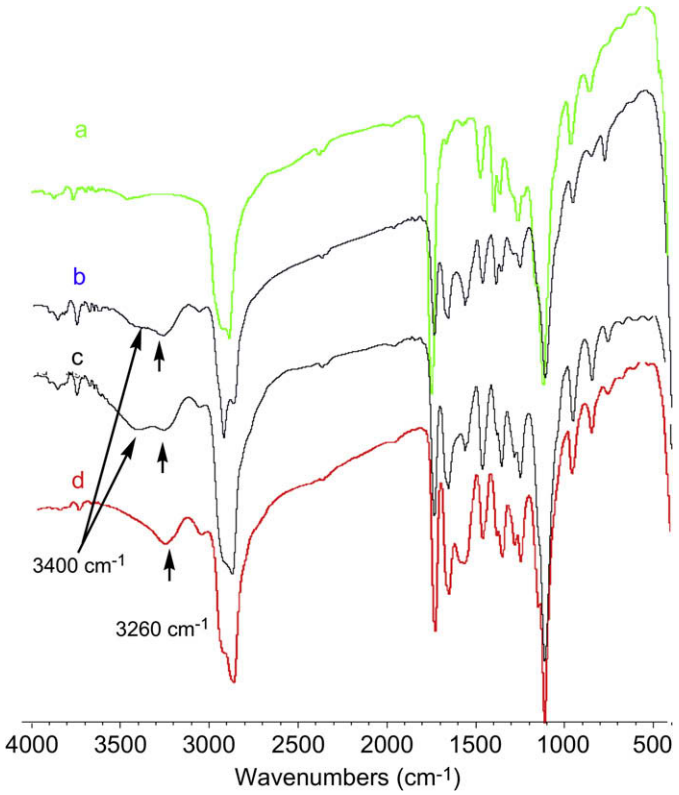

Fig. 2. IR spectra of (a) PEO-*b*-PCCL, (b) PEO-*b*-P(CL-*g*-SP), (c) PEO-*b*-P(CL-*g*-TP) and (d) PEO-*b*-P(CL-*g*-DP).

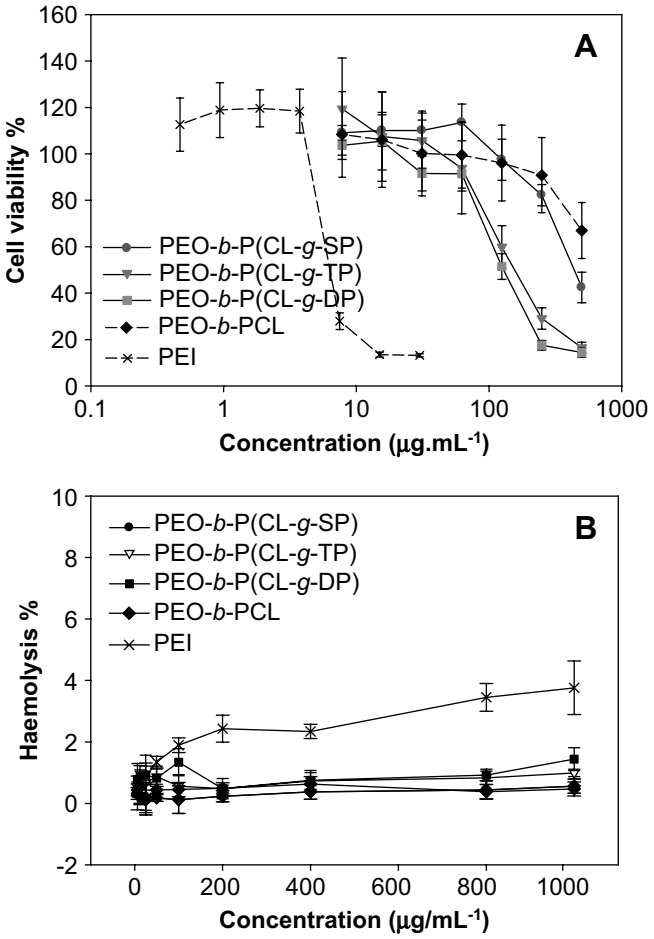

Fig. 3. Cytotoxicity (A) and haemolytic activity (B) of the synthesized PEO-*b*-P(CL-*g*-polyamine) against MDA435/LCC6 resistant cancer cells and RBC cells, respectively.

3.3. siRNA binding and formation of PIC micelles

Agarose gel electrophoresis was utilized to detect complex formation between the synthesized copolymers and the siRNA. This was based on the disappearance of free siRNA bands in the agarose gels. As expected, the synthesized PEO-*b*-P(CL-*g*-polyamine) was capable of effectively binding siRNA, resulting in retardation or disappearance of siRNA bands in agarose gel (Fig. 4A). When the N/P ratios were higher than 10:1, the migration of siRNA was completely retarded for all PEO-*b*-poly(CL-*g*-polyamine) copolymers. The binding ability of the polycationic copolymers were not significantly different from each other, but less than that of PEI as indicated by a significant left shift in binding versus N/P ratio plots (Fig. 4B). There were no obvious differences in siRNA binding capacity among the copolymers, except that PEO-*b*-P(CL-*g*-DP) showed a slightly lower siRNA binding ability in terms of weight ratio (inserted panel in Fig. 4B). The parent PEO-*b*-PCL showed very low siRNA binding at all polymer:siRNA weight ratios tested, and PEI showed complete siRNA binding even at very low polymer:-siRNA weight ratio (<1).

The amphiphilic block copolymer is known to self-assemble into micelles in aqueous solution when the polymer concentration is above its CMC. The formation of PIC micelles of various PEO-*b*-P(CL-*g*-polyamine)s with siRNA was investigated by DLS and ζ-potential measurements (Table 1). The average diameters of the PIC micelles ranged from 57 to 91 nm depending on the copolymer structure. The PIC particles formed from the PEI was significantly larger (590 nm). The ζ-potential of the PIC micelles from the synthesized

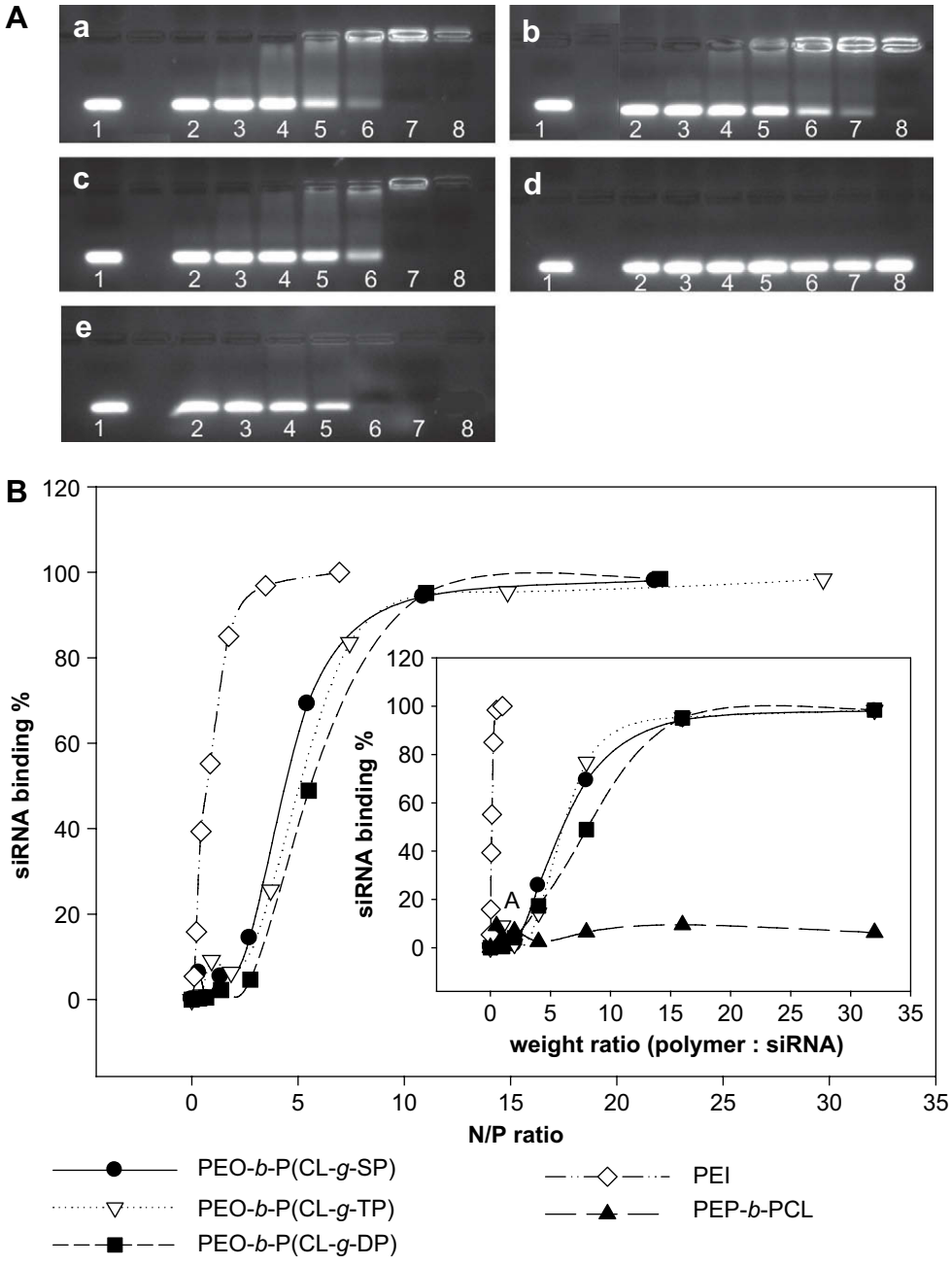

Fig. 4. Electrophoretic retardation analysis of siRNA binding by different polymers. The gel results for the individual polymers are shown in (A). Lane numbers in (A) corresponds to different polymer/siRNA weight ratios for PEO-*b*-P(CL-*g*-SP) (a), PEO-*b*-P(CL-*g*-TP) (b), PEO-*b*-P(CL-*g*-DP) (c), and PEO-*b*-PCL (d): (1) 1:0 (siRNA only), (2) 0.5:1, (3)1:1, (4) 2:1, (5) 4:1, (6) 8:1, (7) 16:1, and (8) 32:1. In the case of PEI (e), the lane numbers correspond to: (1) 1:0 (siRNA only), (2) 0.0155:1, (3) 0.03125:1, (3) 0.0625:1, (4) 0.125:1, (5) 0.25:1, (6) 0.5:1 and (7) 1:1. The densitometric analysis of the binding results is shown in (B). The inserted panel in (B) shows the percentage of siRNA binding versus polymer:siRNA weight ratio.

copolymers were relatively low (2.3–3.3 mV) as compared to the PIC particles formed from PEI (32.7 mV).

3.4. Release of siRNA from polymer/siRNA PIC micelles with polyanion heparin

The siRNA release from various PICs in the presence of heparin is summarized in Fig. 5. The siRNA release from its complex was dependent on heparin concentration. The ratio of heparin to polymer which leads to 50% of siRNA release (RR_{50}) from the complexes was used as a measure of propensity for dissociation. Accordingly, PEO-*b*-P(CL-*g*-SP) and PEO-*b*-P(CL-*g*-TP) formed more stable complexes with siRNA as compared to PEO-*b*-P(CL-*g*-DP), based on the higher RR_{50} values for the former copolymers (0.10 and 0.12 μg/μg, heparin:polymer, respectively) as compared to the RR_{50} value of 0.07 μg/μg, heparin:polymer for PEO-*b*-P(CL-*g*-DP). Complete siRNA release from all PIC micelles was observed when the heparin:polymer weight ratio reached 0.2:1. All the PEO-*b*-(CL-*g*-polyamine)/siRNA complex micelles showed significantly higher siRNA release than the PEI/siRNA complex micelles (RR_{50} = 9.22 μg/μg, heparin:polymer), even though the latter was prepared at the very low polymer:siRNA weight ratio of 1:1.

3.5. Protection of siRNA in PIC micelles from serum degradation

The protective effect of the PIC micelles against siRNA degradation was assessed in serum (Fig. 6). Free siRNA was not stable in 25% FBS and it was completely degraded with 24 h incubation. For the PEO-*b*-P(CL-*g*-polyamine)/siRNA PIC micelles, even the lowest applied polymer:siRNA ratio (8:1) demonstrated a significant protective effect for siRNA where the percentages of intact siRNA in these PIC micelles reached to ~70%. When the ratio is above 16, siRNA was almost fully recoverable and was protected from serum degradation. The synthesized copolymer did not demonstrate a significant difference in the siRNA protection ability.

3.6. Cellular uptake study

FAM-labeled negative siRNA was used to study cellular uptake of siRNA/polymer PIC micelles or PEI/siRNA complexes. Based on flow

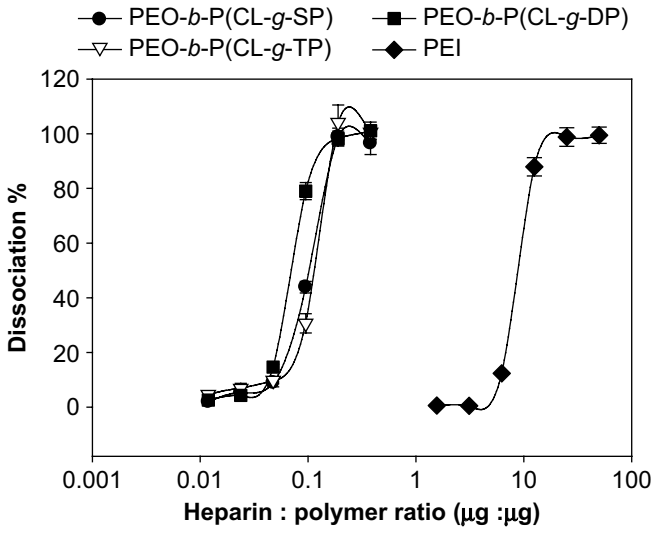

Fig. 5. siRNA dissociation from complexes by heparin competition. siRNA complexed in PEO-*b*-P(CL-*g*-polyamine) with a polymer:siRNA weight ratio of 32:1 and in PEI with a weight ratio of 1:1 were incubated for 1 h at 37 °C with increasing concentrations of polyanionic heparin and amount of complex dissociation was determined assessing free siRNA by agarose gel electrophoresis.

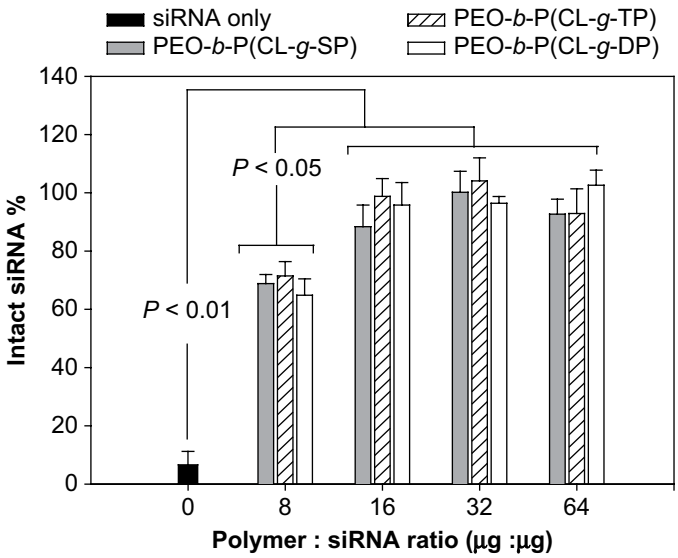

Fig. 6. Determination of siRNA stability in the presence of serum. The data show the percentage of intact siRNA recovered form complexes formed at different polymer:-siRNA weight ratios after incubation of the complexes in 25% serum for 24 h.

cytometry, the cellular uptake of siRNA formulated in various PICs by MDA435/LCC6 cells was in the order of PEI > PEO-*b*-P(CL-*g*-TP) > PEO-*b*-P(CL-*g*-SP) > PEO-*b*-P(CL-*g*-DP) = free siRNA (Fig. 7A and B). The cellular uptake was confirmed with confocal microscopy observation (Fig. 7C). Clear siRNA fluorescence was exclusively observed in cytoplasm when siRNA was formulated in PEO-*b*-P(CL-*g*-SP) or PEO-*b*-P(CL-*g*-TP) micelles as indicated by the red arrows (Fig. 7C-a and C-b, respectively). siRNA formulated in PEO-*b*-P(CL-*g*-DP) micelles (Fig. 7C-c) or siRNA alone (Fig. 7C-d) gave almost no detectable fluorescence in the cells. siRNA formulated in PEI produced large particles with bright fluorescence in cytoplasm as well as in nucleus (Fig. 7C-e). Noticeably, the siRNA appeared to remain in more distinct particles when delivered with the PEI, whereas a more diffuse pattern was evident for the siRNA delivered with the PEI-*b*-(CL-*g*-polyamines).

3.7. Endosome/lysosome escape for siRNA/polymer complex micelles

PEO-*b*-P(CL-*g*-polyamine)s were designed to have protonatable amino groups with pK_as around the endosomal pH, so as to introduce high buffering capacity that will facilitate endosomal/lysosomal escape [11]. The intracellular uptake of the PIC micelles by endocytosis and the subsequent endosome/lysosome escape were investigated and compared to PEI/siRNA PIC particles using confocal microscopy. The typical images of cells treated with PEO-*b*-P(CL-*g*-TP)/siRNA PIC micelles or PEI/siRNA PIC particles are shown in Fig. 8. At 1 h of incubation, a large fraction of PIC micelles or particles were localized in the acidic compartments as indicated by the yellow color in the merged fluorescence image (Panel d) of the FAM-labeled siRNA (green, Panel a) and LysoTracker (red, Panel b), indicating that the PIC micelles or PEI particles were internalized into cells by endocytosis to form endosomes/lysosomes. At 3 h of incubation, a definite fraction of siRNA (green) in the cytoplasm was not co-localized with LysoTracker (red) and the green fluorescence became relatively stronger than the red fluorescence, suggesting that this fraction was located in a compartment other than the acidic endosomes/lysosomes or the endosomes/lysosomes were disrupted. PEO-*b*-P(CL-*g*-SP)/siRNA PIC micelles showed similar results as PEO-*b*-P(CL-*g*-TP)/siRNA micelles did (data not shown). Yellow and green fluorescence were seen at the same slide

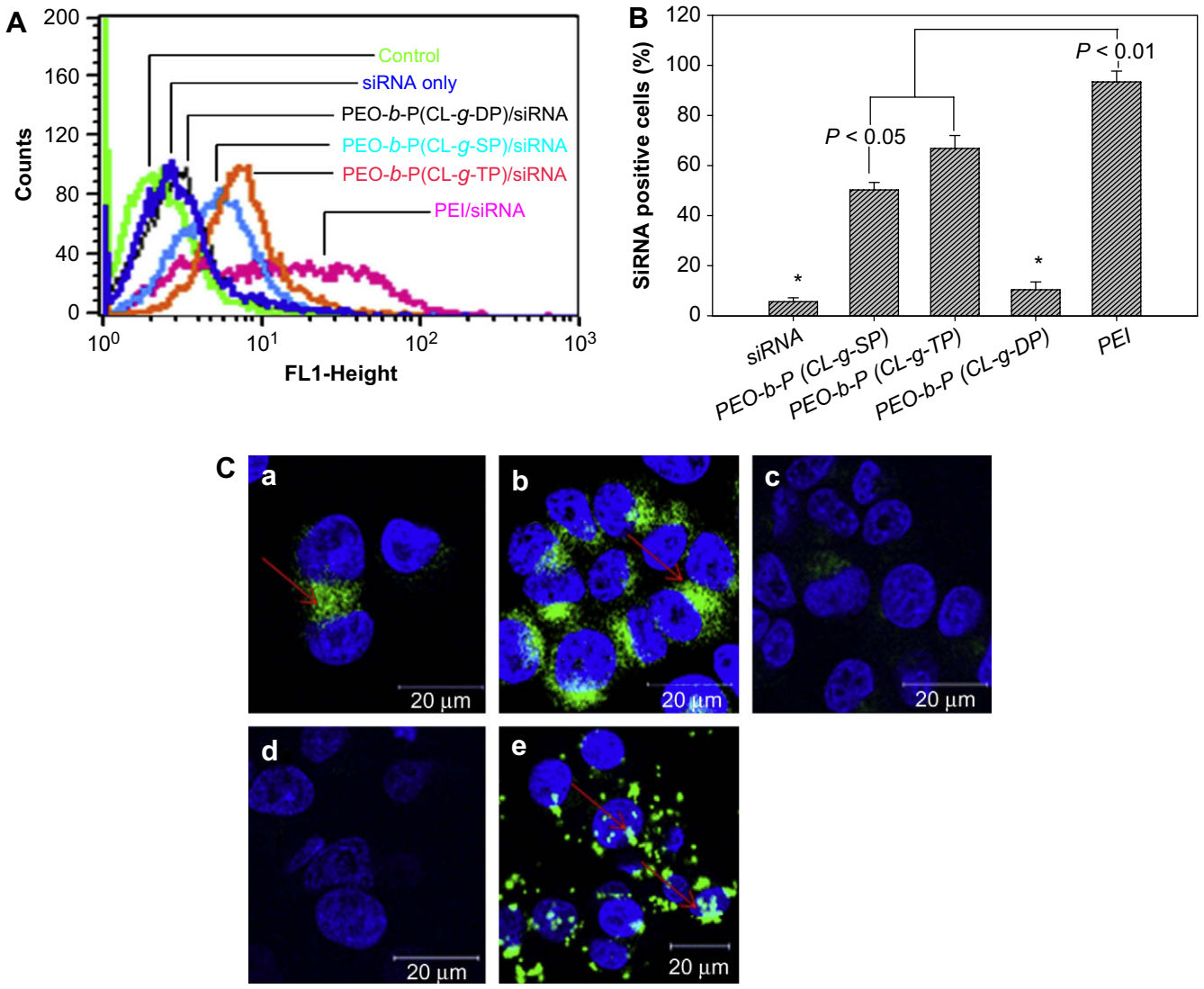

Fig. 7. Cellular uptake of FAM-siRNA from different PIC micelles or from PEI/siRNA PICs by MDA435/LCC6 cells. (A) Flow cytometric histogram profiles of fluorescence intensity for cells treated with siRNA formulated in different polymers. (B) siRNA positive cells after treatment with different FAM-siRNA formulations. The data are the mean ± standard error for $n = 3$. The untreated cells were used as the reference group. $^*P < 0.01$, when siRNA alone and PEO-*b*-P(CL-*g*-DP)/siRNA were compared to PEO-*b*-P(CL-*g*-SP)/siRNA, PEO-*b*-P(CL-*g*-TP)/siRNA and PEI/siRNA. (C) Confocal microscopy images of cells after treatment with FAM-siRNA formulated in (a) PEO-*b*-P(CL-*g*-SP), (b) PEO-*b*-P(CL-*g*-TP), (c) PEO-*b*-P(CL-*g*-DP), (d) HEPES and (e) PEI. The nuclei are stained blue (DAPI) and the internalized siRNA appears as green (FAM). (For interpretation of the references to color in this figure legend, the reader is referred to the web version of this article.)

even after 1 h of incubation for both PEI/siRNA and PEO-*b*-P(CL-*g*-TP)/siRNA complexes (Fig. 8e1 and e2 and f1 and f2) pointing to the efficient and rapid endocytosis and endosome/lysosome escape of both delivery systems. The size of the formed endosomes appeared much larger for PEI delivery system. This is not surprising since the size of endosomes is dependent on the endocytosed particles (570 nm for PEI particles versus 65 nm for PEO-*b*-P(CL-*g*-TP) micelles). The size of endosomes may become larger by fusion of many smaller endosomes which was also observed in our fluorescent microscopy pictures (Fig. 8e3 and f1). A comparison between distribution of green fluorescence (related to complexed siRNA) between cells transfected with PEI and PEO-*b*-P(CL-*g*-TP) micelles either at 1 or 3 h incubation period, reveals a more homogenous distribution of the P(CL-*g*-TP) micelles throughout the cells. This may reflect an easier release of siRNA from its micellar carrier compared to PEI, or be simply due to the smaller size of P(CL-*g*-TP) micelles compared to PEI complexes. It is worthy to note that the timescale of cellular endocytosis to form endosomes and endosome/lysosome escape are very heterogeneous. Endocytosis and endosome/lysosome escape at different phases can occur in same single cell and at same time point (Fig. 8e1–e4 and f1–f4).

3.8. MDR-1 *siRNA silenced P-gp expression on MDA435/LCC6 cells*

The ability of PEO-*b*-P(CL-*g*-SP) and PEO-*b*-P(CL-*g*-TP) to deliver a functional siRNA was evaluated using *MDR-1*-targeted siRNA to inhibit P-gp expression in MDA435/LCC6 cells. PEI was used as a control carrier. The relative P-gp expression levels by cells treated with different concentrations of anti-*MDR-1* or negative siRNA formulations are shown in Fig. 9. Negative siRNA containing formulations failed to inhibit P-gp expression at all concentrations (Fig. 9A). The silencing of P-gp expression was dependent on the concentration of the functional siRNA (Fig. 9B). 100 nM of siRNA in all formulations didn't produce significant inhibition in the P-gp expression. *MDR-1* siRNA (200 nM) formulated in PEO-*b*-P(CL-*g*-SP) or PEO-*b*-P(CL-*g*-TP) micelles was as effective as PEI/*MDR-1* siRNA (1:1 ratio) to inhibit P-gp expression (~20% of P-gp inhibition). When siRNA concentration was

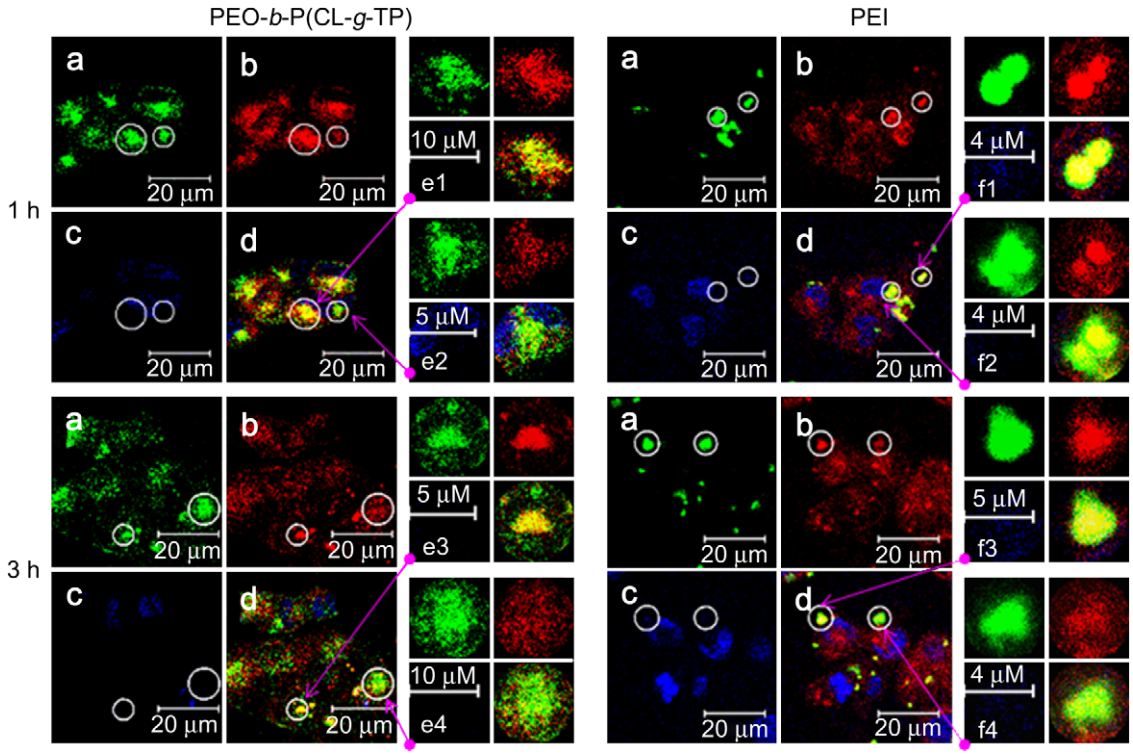

Fig. 8. Assessment of endosomal escape for PEO-*b*-P(CL-*g*-TP) and PEI after intracellular uptake by endocytosis upon 1 and 3 h incubation by confocal microscopy. The cells were treated with FAM-labeled siRNA formulated in PEO-*b*-P(CL-*g*-TP) and PEI (green, panel a); Lysosomes and nuclei were stained by LysoTracker (red, panel b) and DAPI (blue, panel c), respectively, and the images were merged in panel d. The endosomes/lysosomes in cells treated with PCI micelles and particles in different phases were magnified in e and f, respectively. (For interpretation of the references to color in this figure legend, the reader is referred to the web version of this article.)

increased to 300 nM, PEO-*b*-P(CL-*g*-TP)/*MDR-1* siRNA showed significantly higher inhibition of P-gp expression (~60% of P-gp inhibition) than PEO-*b*-P(CL-*g*-SP)/*MDR-1* siRNA complex micelles and PEI/siRNA complex (~50% of P-gp inhibition).

The inhibition of P-gp expression mediated by *MDR-1* siRNA was further observed by confocal microscopy. Fig. 10 shows the fluorescence images of the cells treated with *MDR-1* siRNA or negative siRNA complex (300 nM), and stained with FITC-labeled anti-P-gp monoclonal antibody. PEO-*b*-P(CL-*g*-SP) and PEO-*b*-P(CL-*g*-TP)/*MDR-1* siRNA complex micelles as well as PEI/*MDR-1* siRNA complex resulted in weaker fluorescence (green) on the cell membrane than the cells treated with negative siRNA, confirming that P-gp expression on the cell membrane was effectively inhibited by *MDR-1* siRNA complex micelles.

4. Discussion

In this study, we grafted different polyamine groups to the PCL block of the amphiphilic PEO-*b*-PCL copolymer to obtain a novel family of biodegradable and self-associating polymers with potential for *in vivo* siRNA delivery. Amphiphilic PEO-*b*-polyesters and PEO-*b*-poly(L-amino acid)s (PEO-*b*-PLAA) represent two traditional polymeric biomaterials for self-assembly into micelles for drug delivery *in vivo* [31]. PEO-*b*-PLAAs have demonstrated versatile use both in drug and in gene delivery due to the introduction of functional groups in the PLAA block. PEO-*b*-polyesters such as PEO-*b*-PCL and PEO-*b*-PLGA have been of interest in drug delivery because of their excellent long-term safety profiles in clinical application and lower CMC. However, their use in gene delivery was limited due to the absence of cationic moieties on their structure and untailorable polyester backbone. To encapsulate genetic cargoes such as plasmid DNA or siRNA into the nonionic polyester based particulate carriers, complicated procedures or organic solvents that could denature nucleic acids might be used to attain sufficient loading efficiency [32]. However, due to weak condensation, the nucleic acids tend to be released rapidly from the carriers. In addition, the nucleic acids are more susceptible to nuclease attack since they are not typically condensed in these carriers. Attempts have been made to modify the polyester block with cationic residues that can provide anchoring site for genetic cargoes. To date, most of the modifications were focused on introducing cationic blocks (e.g. PEI or PLL) to the end of polyester homo or block copolymers [33–35]. To our best knowledge, modification of the polyester backbone by introducing cationic side groups on ester repeat unit has not been reported. Owing to the biocompatibility of the PEO shell and biodegradability of the PCL core, the PEO-*b*-P(CL-g-polyamine) PIC micelles prepared in the current study are expected to be safe for *in vivo* administration. Moreover, the biodegradability of the PCL core along with the presence of short polycations in the PEO-*b*-P(CL-*g*-polyamine) PIC micelles are expected to provide the required buffering capacity and osmotic drive required for efficient endosmal escape and expression of the incorporated siRNA.

The developed amphiphilic copolymers were shown to be non-haemolytic and less toxic than PEI against the chosen cancer cell line. They were also shown to be able to effectively bind siRNA, self-assemble into micelles and protect siRNA from degradation by nuclease in serum. The polyamines SP, TP and DP, were grafted to PCL block to provide high density of amine for siRNA binding and protection. However, the substitution is not complete and the presence of unsubstituted carboxyl groups in the PCL block may partly counterbalance their siRNA binding capacity by formation of complexes through electrostatic interactions between the protonated amines and de-protonated carboxyl groups on the PCL block. In addition, grafting of polyamine led to higher CMCs for the copolymers. To assure complete siRNA binding and micelle

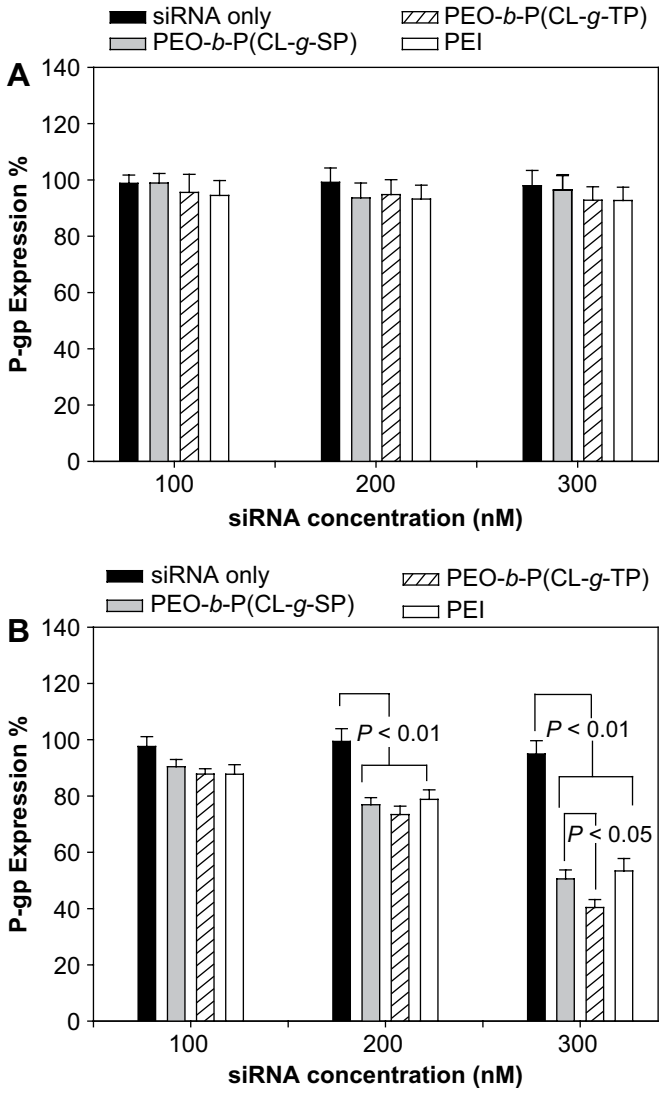

Fig. 9. Polymer/*MDR-1* siRNA mediated P-gp gene silencing in MDA435/LCC6 cells. Cells treated with (A) negative siRNA formulated in various polymers and (B) *MDR-1*-targeted siRNA formulated in various polymers for 48 h at 37 °C. The P-gp expression was analyzed by flow cytometry and results are reported as mean fluorescence ± SD for triplicate samples.

formation, the PIC micelles were prepared at a high polymer:-siRNA weight ratio (32:1), which is equivalent to N/P ratios of 20–29. The prepared PEO-*b*-P(CL-*g*-polyamine)/siRNA complexes was shown to form micelle with a particle size <100 nm and relatively neutral surfaces (~3.0 mV) pointing to the effectiveness of PEO in shielding the cationic core charge [36,37]. This is in contrast to PEI/siRNA complexes that displayed a particle size of 570 nm with positively charged surfaces (+32.7 mV). More importantly, siRNA formulated in the developed PIC micelles was well protected against nuclease degradation and it maintained its integrity up to 24 h after incubation in 25% serum. This is comparable to the siRNA protective effect of PEI. The resistance to nuclease degradation is essential for a successful siRNA delivery both *in vitro* and in particular *in vivo*. siRNA is highly susceptible to nuclease as evidenced by the degradation results in this study, where more than 90% of free siRNA were destroyed in 25% serum within 4 h of incubation (Fig. 6) [38].

The cellular uptake of micelles is assumed to be dependent on the micellar shell which directly interfaces the cells. Other parameters such as the nature of the cells, the micelle core, and micelle particle size may also affect their cellular uptake [39–42]. We found that amphiphilic polycationic polymers with primary amine end (e.g. SP and TP) in their core-forming structures were more efficient for siRNA cellular uptake compared to polymers with tertiary amine end (DP) (Fig. 7). The increased association of the SP and TP containing PIC micelles with siRNA may explain the reason behind facilitated cellular uptake of siRNA by these structures [42]. There is a possibility for the folding of the amine groups grafted on the polyester as a result of formation of hydrogen bonds between them and oxygen on the PEO block [43], leading to the insertion of the polyamine-grafted polyester block into the micellar shell. Moreover, given the reported structural effects of polyamine on cellular internalization [44], a contribution from exposure of primary amines in PEO-*b*-P(CL-*g*-SP) or PEO-*b*-P(CL-*g*-TP) unimers in increasing the cellular uptake siRNA can be speculated. Finally, a larger particle size might have attributed to the lower cellular uptake of PEO-*b*-P(CL-*g*-DP)/siRNA micelles compared to PEO-*b*-P(CL-*g*-SP)/siRNA or PEO-*b*-P(CL-*g*-TP)/siRNA micelles.

Another distinctive function of grafting polyamine groups to PCL block is that these polyamine molecules contain protonatable amino groups with different pK_as, which are designed to introduce high buffering capacity for membrane disruption that will facilitate endosomal/lysosomal escape [11,45]. Confocal images further revealed that PEO-*b*-P(CL-*g*-SP) and PEO-*b*-P(CL-*g*-TP) can specifically deliver the siRNA into cytoplasm, whereas siRNA delivered by PEI was found to be in cytoplasm as well as in the nucleus (Fig. 7C). Accumulation of siRNA in the cytoplasm where its target mRNA locates (rather than nucleus) provides another advantage for the developed PEO-*b*-P(CL-*g*-polyamine)s over PEI for siRNA delivery [46]. The specific cytoplasmic delivery of siRNA might be attributed to greater propensity of siRNA to dissociate when complexed by PEO-*b*-P(CL-*g*-polyamine)s. The nucleus trafficking of genetic cargoes delivered by PEI based carrier was also observed by others [47–49]. PEI with high charge density would efficiently condense siRNA to form tightly compact complexes, which remain intact after cellular internalization, endosomal/lysosomal escape, and may then enter the nucleus together with its siRNA cargo. However, due to lower amine density and the presence of unsubstituted carboxyl group, PEO-*b*-P(CL-*g*-SP) or PEO-*b*-(CL-*g*-DP) could form loosely compact complex, and the complexed siRNA might dissociate from the polymer before or after endosome escape, limiting its localization to the cytoplasm. The biodegradability of the PCL core may also assist in this process. The different morphology of fluorescence in cells also suggests a possibility for different siRNA compaction leading to changes in siRNA intracellular trafficking for PEI as compared to PEO-*b*-P(CL-*g*-polyamine) PIC micelles (Fig. 4A).

The endocytosis and endosome escape of PEO-*b*-P(CL-*g*-SP)/siRNA and PEO-*b*-P(CL-*g*-TP)/siRNA after cellular uptake were further confirmed by confocal microscopic observations (Fig. 8). Although the theory of proton sponge hypothesis is still arguable [50], it has been extensively used to design effective carriers for delivery of genetic cargoes [11,45]. The pH-sensitive cell membrane disruption of siRNA carriers composed of polyamine has well been evidenced and proved to be directly related to their cellular siRNA delivery efficiency [45,51]. Micellar structures based on PEO-*b*-PLAA with attached polyamine groups were endowed ability for endosome escape and have displayed impressive gene knockdown activity *in vitro* [11]. Consistent with these findings, we have seen a correlation between efficient endocytosis, endosomal escape and efficient gene silencing by siRNA micelles (Figs. 8–10).

Multidrug resistance, which is commonly caused by overexpression of P-gp encoded by *MDR-1*, has been one of the major causes of the failure of chemotherapy in cancer patients [52,53]. Modulations of multidrug resistance by pharmaceutical agents,

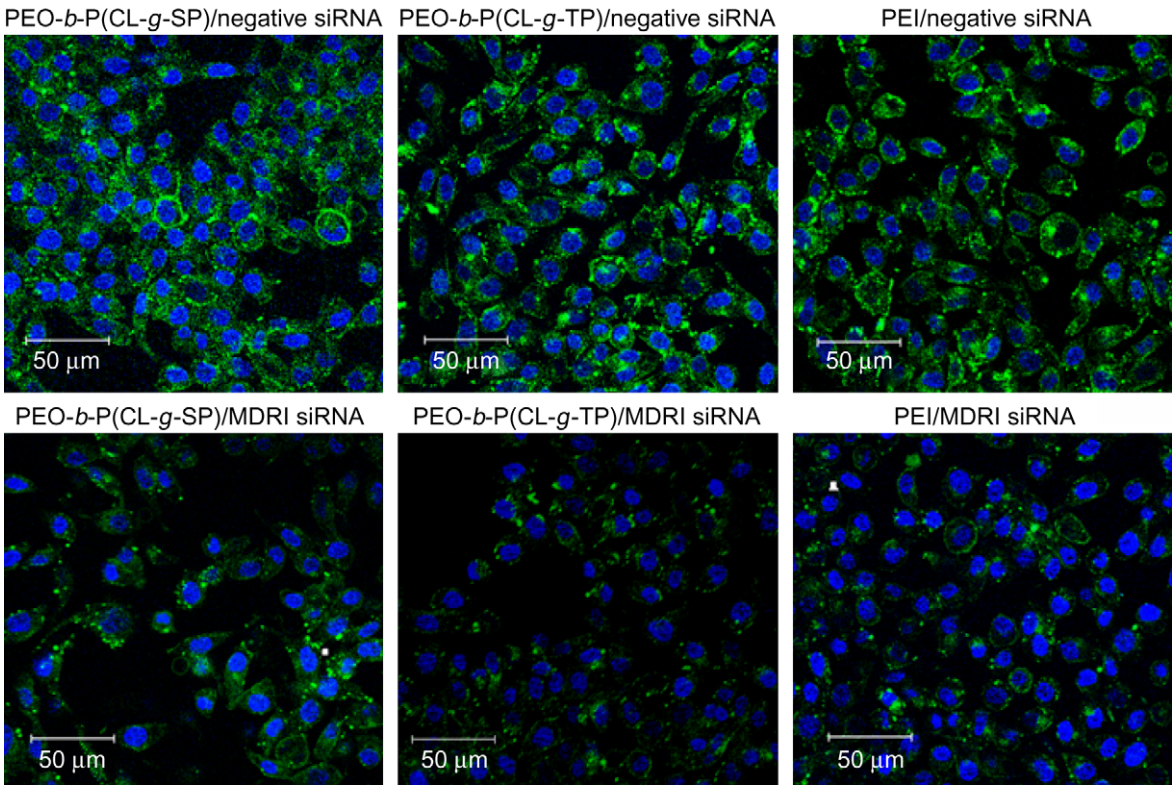

Fig. 10. Fluorescence images of MDA435/LCC6 resistant cells transfected with 300 nM of *MDR-1* siRNA or negative siRNA formulated in PEO-*b*-P(CL-*g*-SP), PEO-*b*-P(CL-*g*-TP) and PEI complex. The cells were stained with FITC-labeled P-gp antibody (green) and DAPI (blue) for P-gp and nuclei staining, respectively.

antibodies, antisense oligonucleotides, and inhibitors of signal transduction have been pursued either by inhibition of P-gp activity or by inhibition of P-gp expression. The clinical benefit of these approaches remains to be realized, however [54–56]. RNAi mediated gene silencing was shown to be specific and potent, and it has been applied to overcome P-gp mediated MDR in different *in vitro* models [54,57]. *MDR-1* siRNA formulated in PEO-*b*-P(CL-*g*-polyamine) micelles would provide better chances for tumor-targeted delivery of siRNA through systemic administration. In this *in vitro* evaluation, we found that the polymeric formulations mediate siRNA silencing of P-gp in a dose-dependent manner in MDA435/LCC6 cells. PEO-*b*-P(CL-*g*-TP)/*MDR-1* siRNA (300 nM) showed higher P-gp expression inhibition than PEO-*b*-P(CL-*g*-SP)/*MDR-1* siRNA (300 nM), which may be caused by the higher cellular uptake of *MDR-1* siRNA when formulated in PEO-*b*-P(CL-*g*-TP) micelles. It is not surprising that higher cellular uptake of *MDR-1* siRNA formulated with PEI did not demonstrate any improved P-gp silencing compared to *MDR-1* siRNA formulated in PEO-*b*-P(CL-*g*-SP) or PEO-*b*-P(CL-*g*-TP) micelles, since siRNA formulated PEO-*b*-P(CL-*g*-polyamine) micelles appeared to be more efficiently released from complex micelles after cellular uptake. Despite a high concentration of *MDR-1* siRNA (300 nM), the maximum inhibition of P-gp expression was <60% for all the *MDR-1* siRNA formulations. The lack of complete inhibition is likely due to the high content of P-gp in the chosen cell line (since these cells are transfected for overexpression of P-gp), and the transient duration of P-gp gene silencing effect [58]. The extent of P-gp inhibition remains to be seen in more primary cell lines that express clinical levels of P-gp. A further increase in the siRNA concentration may lead to complete P-gp gene silencing, but will increase the risk of off-target suppression of other genes due to the sequence similarity [59]. Finally since P-gp is also expressed in normal tissues such as blood brain barrier, its non-selective silencing may lead to complications and toxicity by P-gp substrate. Using cancer specific targeting ligands to modify the polycationic micelles is expected to increase the silencing efficiency more selectively in cancerous cells rather than normal cells that express P-gp [60]. Targeted siRNA delivery to silence P-gp gene expression and evaluation of the effect on sensitivity of MDR cells to anticancer drugs are underway in our research group.

5. Conclusions

In conclusion, we report on the design, synthesis and evaluation of a novel family of PEO-*b*-polyester based polycationic copolymers and explored their potential for siRNA delivery. We demonstrated that all these amphiphilic polycationic copolymers can effectively bind siRNA, self-assemble into micelles and protect siRNA from degradation by nuclease in serum. PEO-*b*-P(CL-*g*-SP) and PEO-*b*-P(CL-*g*-TP) micelles in particular can efficiently deliver siRNA into cytoplasm by endocytosis and facilitate endosome escape after cellular uptake. *MDR-1*-targeted siRNA formulated in PEO-*b*-P(CL-*g*-SP) and PEO-*b*-P(CL-*g*-TP) exhibited efficient gene silencing for P-gp expression. The synthetic amphiphilic PEO-*b*-P(CL-*g*-polyamine) block copolymers present a promising efficient carrier for siRNA delivery especially for systemic administration.

Acknowledgements

This research was funded by research grants from Natural Science and Engineering Research Council of Canada (NSERC) and Canadian Institute of Health Research (CIHR).

Appendix

Figures with essential colour discrimination. Certain figures in this article, particularly Figures 8 and 10, are difficult to interpret in

black and white. The full colour images can be found in the on-line version, at doi:10.1016/j.biomaterials.2008.09.025.

References

[1] de Fougerolles A, Vornlocher HP, Maraganore J, Lieberman J. Interfering with disease: a progress report on siRNA-based therapeutics. Nat Rev Drug Discov 2007;6:443–53.
[2] Iorns E, Lord CJ, Turner N, Ashworth A. Utilizing RNA interference to enhance cancer drug discovery. Nat Rev Drug Discov 2007;6:556–68.
[3] Wall NR, Shi Y, Small RNA. Can RNA interference be exploited for therapy? The Lancet 2003;362:1401–3.
[4] Blow N. Small RNAs: delivering the future. Nature 2007;450:1117–20.
[5] Ryther RC, Flynt AS, Phillips 3rd JA, Patton JG. siRNA therapeutics: big potential from small RNAs. Gene Ther 2005;12:5–11.
[6] Aigner A. Applications of RNA interference: current state and prospects for siRNA-based strategies in vivo. Appl Microbiol Biotechnol 2007;76:9–21.
[7] Aagaard L, Rossi JJ. RNAi therapeutics: principles, prospects and challenges. Adv Drug Deliv Rev 2007;59:75–86.
[8] Haupenthal J, Baehr C, Zeuzem S, Piiper A. RNAse A-like enzymes in serum inhibit the anti-neoplastic activity of siRNA targeting polo-like kinase 1. Int J Cancer 2007;121:206–10.
[9] Kumar LD, Clarke AR. Gene manipulation through the use of small interfering RNA (siRNA): from in vitro to in vivo applications. Adv Drug Deliv Rev 2007;59:87–100.
[10] Gary DJ, Puri N, Won YY. Polymer-based siRNA delivery: perspectives on the fundamental and phenomenological distinctions from polymer-based DNA delivery. J Controlled Release 2007;121:64–73.
[11] Itaka K, Kanayama N, Nishiyama N, Jang WD, Yamasaki Y, Nakamura K, et al. Supramolecular nanocarrier of siRNA from PEG-based block catiomer carrying diamine side chain with distinctive p*K*(a) directed to enhance intracellular gene silencing. J Am Chem Soc 2004;126:13612–3.
[12] Kim SH, Jeong JH, Cho KC, Kim SW, Park TG. Target-specific gene silencing by siRNA plasmid DNA complexed with folate-modified poly(ethylenimine). J Controlled Release 2005;104:223–32.
[13] Lee SH, Kim SH, Park TG. Anticancer effect by intratumoral and intravenous administration of VEGF siRNA polyelectrolyte complex micelles. J Biotechnol 2007;131:S48–9.
[14] Nishiyama N, Kataoka K. Current state, achievements, and future prospects of polymeric micelles as nanocarriers for drug and gene delivery. Pharmacol Ther 2006;112:630–48.
[15] Sato A, Choi SW, Hirai M, Yamayoshi A, Moriyarna R, Yamano T, et al. Polymer brush-stabilized polyplex for a siRNA carrier with long circulatory half-life. J Controlled Release 2007;122:209–16.
[16] Aliabadi HM, Brocks DR, Lavasanifar A. Polymeric micelles for the solubilization and delivery of cyclosporine A: pharmacokinetics and biodistribution. Biomaterials 2005;26:7251–9.
[17] Zweers ML, Engbers GH, Grijpma DW, Feijen J. Release of anti-restenosis drugs from poly(ethylene oxide)–poly(DL-lactic-*co*-glycolic acid) nanoparticles. J Controlled Release 2006;114:317–24.
[18] Ruan G, Feng S-S. Preparation and characterization of poly(lactic acid)–poly(ethylene glycol)–poly(lactic acid) (PLA–PEG–PLA) microspheres for controlled release of paclitaxel. Biomaterials 2003;24:5037–44.
[19] Harris JM, Chess RB. Effect of pegylation on pharmaceuticals. Nat Rev Drug Discov 2003;2:214–21.
[20] Chinol M, Casalini P, Maggiolo M, Canevari S, Omodeo ES, Caliceti P, et al. Biochemical modifications of avidin improve pharmacokinetics and biodistribution, and reduce immunogenicity. Br J Cancer 1998;78:189–97.
[21] Amsden BG, Tse MY, Turner ND, Knight DK, Pang SC. In vivo degradation behavior of photo-cross-linked star-poly(ε-caprolactone-*co*-D,L-lactide) elastomers. Biomacromolecules 2006;7:365–72.
[22] Athanasiou KA, Niederauer GG, Agrawal CM. Sterilization, toxicity, biocompatibility and clinical applications of polylactic acid/polyglycolic acid copolymers. Biomaterials 1996;17:93–102.
[23] Ravi Kumar MNV, Bakowsky U, Lehr CM. Preparation and characterization of cationic PLGA nanospheres as DNA carriers. Biomaterials 2004;25:1771–7.
[24] Scott ND, Walker JF, Hansley VL. Sodium naphthalene. I A new method for the preparation of addition compounds of alkali metals and polycyclic aromatic hydrocarbons. J Am Chem Soc 1936;58:2442–4.
[25] Leonessa F, Green D, Licht T, Wright A, Wingate-Legette K, Lippman J, et al. MDA435/LCC6 and MDA435/LCC6MDR1: ascites models of human breast cancer. Br J Cancer 1996;73:154–61.
[26] Wong HL, Bendayan R, Rauth AM, Xue HY, Babakhanian K, Wu XY. A mechanistic study of enhanced doxorubicin uptake and retention in multidrug resistant breast cancer cells using a polymer–lipid hybrid nanoparticle system. J Pharmacol Exp Ther 2006;317:1372–81.
[27] Mahmud A, Xiong XB, Lavasanifar A. Novel self-associating poly(ethylene oxide)-*block*-poly(epsilon-caprolactone) block copolymers with functional side groups on the polyester block for drug delivery. Macromolecules 2006;39:9419–28.
[28] Cayot P, Tainturier G. The quantification of protein amino groups by the trinitrobenzenesulfonic acid method: a reexamination. Anal Biochem 1997;249:184–200.
[29] Merdan T, Callahan J, Petersen H, Kunath K, Bakowsky U, Kopeckova P, et al. Pegylated polyethylenimine-Fab' antibody fragment conjugates for targeted gene delivery to human ovarian carcinoma cells. Bioconjug Chem 2003;14:989–96.
[30] Lavasanifar A, Samuel J, Kwon GS. The effect of alkyl core structure on micellar properties of poly(ethylene oxide)-block-poly(L-aspartamide) derivatives. Colloids Surf B Biointerfaces 2001;22:115–26.
[31] Lavasanifar A, Samuel J, Sattari S, Kwon GS. Block copolymer micelles for the encapsulation and delivery of amphotericin B. Pharm Res 2002;19:418–22.
[32] Cohen-Sacks H, Najajreh Y, Tchaikovski V, Gao G, Elazer V, Dahan R, et al. Novel PDGFbetaR antisense encapsulated in polymeric nanospheres for the treatment of restenosis. Gene Ther 2002;9:1607–16.
[33] Shuai X, Merdan T, Unger F, Kissel T. Supramolecular gene delivery vectors showing enhanced transgene expression and good biocompatibility. Bioconjug Chem 2005;16:322–9.
[34] Arote R, Kim TH, Kim YK, Hwang SK, Jiang HL, Song HH, et al. A biodegradable poly(ester amine) based on polycaprolactone and polyethylenimine as a gene carrier. Biomaterials 2007;28:735–44.
[35] Jang JS, Kim SY, Lee SB, Kim KO, Han JS, Lee YM. Poly(ethylene glycol)/poly (epsilon-caprolactone) diblock copolymeric nanoparticles for non-viral gene delivery: the role of charge group and molecular weight in particle formation, cytotoxicity and transfection. J Controlled Release 2006;113:173–82.
[36] Ogris M, Brunner S, Schuller S, Kircheis R, Wagner E. PEGylated DNA/transferrin-PEI complexes: reduced interaction with blood components, extended circulation in blood and potential for systemic gene delivery. Gene Ther 1999;6:595–605.
[37] Itaka K, Yamauchi K, Harada A, Nakamura K, Kawaguchi H, Kataoka K. Polyion complex micelles from plasmid DNA and poly(ethylene glycol)–-poly(L-lysine) block copolymer as serum-tolerable polyplex system: physicochemical properties of micelles relevant to gene transfection efficiency. Biomaterials 2003;24:4495–506.
[38] Harada-Shiba M, Yamauchi K, Harada A, Takamisawa I, Shimokado K, Kataoka K. Polyion complex micelles as vectors in gene therapy – pharmacokinetics and in vivo gene transfer. Gene Ther 2002;9:407–14.
[39] Maysinger D, Berezovska O, Savic R, Soo PL, Eisenberg A. Block copolymers modify the internalization of micelle-incorporated probes into neural cells. Biochim Biophys Acta 2001;1539:205–17.
[40] Deshpande MC, Davies MC, Garnett MC, Williams PM, Armitage D, Bailey L, et al. The effect of poly(ethylene glycol) molecular architecture on cellular interaction and uptake of DNA complexes. J Controlled Release 2004;97:143–56.
[41] Mahmud A, Lavasanifar A. The effect of block copolymer structure on the internalization of polymeric micelles by human breast cancer cells. Colloids Surf B Biointerfaces 2005;45:82–9.
[42] Miyata K, Fukushima S, Nishiyama N, Yamasaki Y, Kataoka K. PEG-based block catiomers possessing DNA anchoring and endosomal escaping functions to form polyplex micelles with improved stability and high transfection efficacy. J Controlled Release 2007;122:252–60.
[43] Borg J, Jensen MH, Sneppen K, Tiana G. Hydrogen bonds in polymer folding. Phys Rev Lett 2001;86:1031–3.
[44] Liu Y, Reineke TM. Poly(glycoamidoamine)s for gene delivery. structural effects on cellular internalization, buffering capacity, and gene expression. Bioconjug Chem 2007;18:19–30.
[45] Wang XL, Ramusovic S, Nguyen T, Lu ZR. Novel polymerizable surfactants with pH-sensitive amphiphilicity and cell membrane disruption for efficient siRNA delivery. Bioconjug Chem 2007;18:2169–77.
[46] Song J-J, Smith SK, Hannon GJ, Joshua-Tor L. Crystal structure of argonaute and its implications for RISC slicer activity crystal structure of argonaute and its implications for RISC slicer activity. Science 2004;305:1434–7.
[47] Farrell LL, Pepin J, Kucharski C, Lin X, Xu Z, Uludag H. A comparison of the effectiveness of cationic polymers poly-L-lysine (PLL) and polyethylenimine (PEI) for non-viral delivery of plasmid DNA to bone marrow stromal cells (BMSC). Eur J Pharm Biopharm 2007;65:388–97.
[48] Clements BA, Incani V, Kucharski C, Lavasanifar A, Ritchie B, Uludag H. A comparative evaluation of poly-L-lysine-palmitic acid and Lipofectamine 2000 for plasmid delivery to bone marrow stromal cells. Biomaterials 2007;28:4693–704.
[49] Pollard H, Remy JS, Loussouarn G, Demolombe S, Behr JP, Escande D. Polyethylenimine but not cationic lipids promotes transgene delivery to the nucleus in mammalian cells. J Biol Chem 1998;273:7507–11.
[50] Funhoff AM, van Nostrum CF, Koning GA, Schuurmans-Nieuwenbroek NM, Crommelin DJ, Hennink WE. Endosomal escape of polymeric gene delivery complexes is not always enhanced by polymers buffering at low pH. Biomacromolecules 2004;5:32–9.
[51] Wang XL, Nguyen T, Gillespie D, Jensen R, Lu ZR. A multifunctional and reversibly polymerizable carrier for efficient siRNA delivery. Biomaterials 2008;29:15–22.
[52] Riordan JR, Deuchars K, Kartner N, Alon N, Trent J, Ling V. Amplification of P-glycoprotein genes in multidrug-resistant mammalian cell lines. Nature 1985;316:817–9.
[53] Ueda K, Cardarelli C, Gottesman MM, Pastan I. Expression of a full-length cDNA for the human ''MDR1'' gene confers resistance to colchicine, doxorubicin, and vinblastine. Proc Natl Acad Sci U S A 1987;84:3004–8.
[54] Lage H. MDR1/P-glycoprotein (ABCB1) as target for RNA interference-mediated reversal of multidrug resistance. Curr Drug Targets 2006;7:813–21.

[55] Ford JM, Yang JM, Hait WN. P-glycoprotein-mediated multidrug resistance: experimental and clinical strategies for its reversal. Cancer Treat Res 1996;87:3–38.
[56] Nobili S, Landini I, Giglioni B, Mini E. Pharmacological strategies for overcoming multidrug resistance. Curr Drug Targets 2006;7:861–79.
[57] Li X, Li JP, Yuan HY, Gao X, Qu XJ, Xu WF, et al. Recent advances in P-glycoprotein-mediated multidrug resistance reversal mechanisms. Methods Find Exp Clin Pharmacol 2007;29:607–17.
[58] Wu H, Hait WN, Yang JM. Small interfering RNA-induced suppression of MDR1 (P-glycoprotein) restores sensitivity to multidrug-resistant cancer cells. Cancer Res 2003;63:1515–9.
[59] Jackson AL, Bartz SR, Schelter J, Kobayashi SV, Burchard J, Mao M, et al. Expression profiling reveals off-target gene regulation by RNAi. Nat Biotechnol 2003;21:635–7.
[60] Ikeda Y, Taira K. Ligand-targeted delivery of therapeutic siRNA. Pharm Res 2006;23:1631–40.